

Assessing the applicability of Gassmann's fluid substitution equation for CO₂ storage in underground reservoir rocks

Fabien Allo and Jorge Nustes Andrade, Viridien, Lev Vernik, University of Houston

Summary

Gassmann's equation is routinely used for fluid substitution in elastic and seismic forward modeling applications. Although several alternatives exist, they are more complex and less practical, hence the popularity of Gassmann's equation. But this equation comes with underlying assumptions so checking that it is applicable for any given rock should always be part of the modeling workflow. After discussing Gassmann's theory main limitations, we compare the saturated rock bulk moduli computed with Gassmann's equation and the more general Brown & Korringa's equation to assess the applicability of Gassmann's equation for reservoir rocks used for CO₂ storage. A simple metric, obtainable from dry rock velocity measurements only, is proposed to easily assess Gassmann's applicability and guide the choice of fluid substitution option based on the required modeling accuracy. Illustrations of the magnitude of Gassmann's inaccuracy is provided using data from the Northern Lights sequestration project in the North Sea.

Limitations of Gassmann's equation and practical alternative for more accurate fluid substitution in most reservoir rocks

Most rock physics models rely on Gassmann's equation for computing the bulk modulus of a saturated reservoir rock (K_{ud}) from the bulk moduli of the dry rock (K_d), the pore fluid (K_f) and the solid material that makes up the mineral matrix (K_m). A well-known form of this equation is:

$$K_{ud} = K_d + \beta^2 \left[\frac{\phi}{K_f} + \frac{\beta - \phi}{K_m} \right]^{-1} \quad (1)$$

where ϕ is the total porosity, and β is the Biot coefficient defined as $\beta = 1 - K_d/K_m$. Amongst several restrictions, the following ones are usually considered the most important when assessing the applicability of Gassmann's relation: low seismic frequencies are assumed so that pore pressures are equilibrated throughout the pore space; all the minerals making up the matrix solid material are linearly elastic and have the same bulk and shear moduli; the rock is isotropic; the rock is completely saturated with low viscosity fluid. Although challenged by several experimental results on rocks with complex pore space geometries, Gassmann's equation is often assumed to be independent of the pore space microstructure and, therefore, applicable to any compositionally micro-homogeneous rock (Mavko et al., 2009). This concept was questioned again theoretically in recent papers by Thomsen (2020, 2021), who suggested that more accurate but less practical models, such as those by Biot (1941) and Brown and Korringa (1975) must be used for rocks with

complex pore space geometries. These models consider four independent moduli instead of only the three (K_d , K_f and K_m) used in Gassmann's equation. For instance, Brown and Korringa (1975) derive K_{ud} from the unjacketed saturated rock bulk modulus (K_M) and unjacketed solid material bulk modulus (K'_m). Their equation in its general form can be written as:

$$K_{ud} = K_d + \psi^2 \left[\frac{\phi}{K_f} + \frac{1-\phi}{K'_m} + \frac{\psi-1}{K_M} \right]^{-1} \quad (2)$$

where ϕ is the total porosity, and ψ is the bulk volume effective pressure coefficient defined as $\psi = 1 - K_d/K_M$ (Müller and Sahay, 2016). Brown and Korringa (1975) argue that their model reduces to Gassmann's equation in the case of a compositionally micro-homogeneous rock, which is assumed synonymous to a monomineralic rock, or a rock composed of minerals with similar elastic properties. Indeed, if $K_M = K'_m = K_m$, then equation 2 reduces to equation 1.

The need to evaluate K_M and K'_m instead of just K_m makes B-K's equation less practical than Gassmann's equation. Indeed, unlike K_m that is well approximated by the weighted average of the mineral components of the rock, K_M and K'_m can only be indirectly inferred from laboratory measurements. Both Müller and Sahay (2014) and Thomsen (2020) suggest deriving K_M from Skempton's coefficient, the ratio of undrained fluid pressure to confining pressure measurable in a quasi-static laboratory experiment. But, as of today, this type of experiment remains challenging, expensive, and often inconclusive (Duranti, 2018). Importantly, Thomsen also hints that K_M may depend on the effective stress and microgeometry of the rock, which leads us to consider this parameter and its impact on fluid substitution modeling in the framework of the Vernik-Kachanov (V-K) model. A convenient feature of this rock-physics model, inherited from the Mori-Tanaka effective field theory, is the decoupling between the compliance contributions of pores, driven by the volumetric and deviatoric strain concentration factors (Kachanov et al., 1994) commonly known as pore shape factors, and the compliance contribution of cracks modeled via a stress-dependent crack density term. The V-K model for consolidated sediments (e.g., sandstones and limestones) yields the dry rock moduli as (Vernik, 2016):

$$K_d = K_m \left[1 + \frac{p\phi}{1-\phi} + A(v_m)\eta_0 \frac{\exp(-d\sigma)}{1-\phi} \right]^{-1} \quad (3a)$$

$$G_d = G_m \left[1 + \frac{q\phi}{1-\phi} + B(v_m)\eta_0 \frac{\exp(-d\sigma)}{1-\phi} \right]^{-1} \quad (3b)$$

where p and q are the pore shape factors for bulk and shear modulus respectively, $A(v_m)$ and $B(v_m)$ are known functions of the Poisson's ratio of the solid material (e.g., Benveniste, 1987),

η_0 is the initial or zero-stress crack density, d is the crack aspect ratio distribution-dependent coefficient, which, based on laboratory measurement of velocity vs. stress on dry sandstones and carbonates, generally varies between 0.05 and 0.07, and σ is the effective stress. The third term in equations 3 corresponds to the compliance contribution of cracks. The crack density parameter $\eta = \eta_0 \exp(-d\sigma)$ can vary from zero with no stress sensitivity to as high as 3. However, even rocks with intermediate η values between 0.1 and 0.3 may exhibit significant stress sensitivity of their P- and S-wave velocities. Practically, the zero-stress crack density η_0 can be constrained as a linear function of porosity in sandstones and carbonates using $\eta_0 = c_1 + c_2\phi$ with c_1 ranging between 0.02 and 0.25 and c_2 usually around 2 (Vernik, 2016).

Assuming equations 3 are appropriate to model the dry rock moduli of a micro-heterogeneous rock with cracks, we suggest that the following equations can be used to express theunjacketed bulk modulus and unjacketed solid material bulk modulus of such a rock as a function of measurable effective stress and quantifiable crack density:

$$K_M = K_m \left[1 + A(v_m) \eta_0 \exp(-d\sigma) \right]^{-1} \quad (4a)$$

$$K'_m = \lim_{\phi \rightarrow 0} (K_M) = K_m \left[1 + A(v_m) c_1 \exp(-d\sigma) \right]^{-1} \quad (4b)$$

where c_1 is the intercept of the linear function of porosity used to model η_0 . A direct consequence of using equations 4 in the practical application of B-K's equation is the ability to account for the high stress-sensitivity of rocks with cracks unlike Gassmann's equation which rely on the assumption that K_d converges towards K_m as porosity tends to 0. Figure 1 illustrates how this hypothesis, when unmet, can lead to a substantial overestimation of the saturated rock bulk modulus with Gassmann's equation compared to B-K's equation for a rock with an average crack density subject to a relatively low effective stress (commonly observed in overpressured formations). The figure clearly highlights a substantial difference between the two predictions that reaches a maximum when total porosity is reduced to crack porosity only. Further numerical tests show that this overestimation also augments with increasing crack density, decreasing effective stress and decreasing pore fluid compressibility.

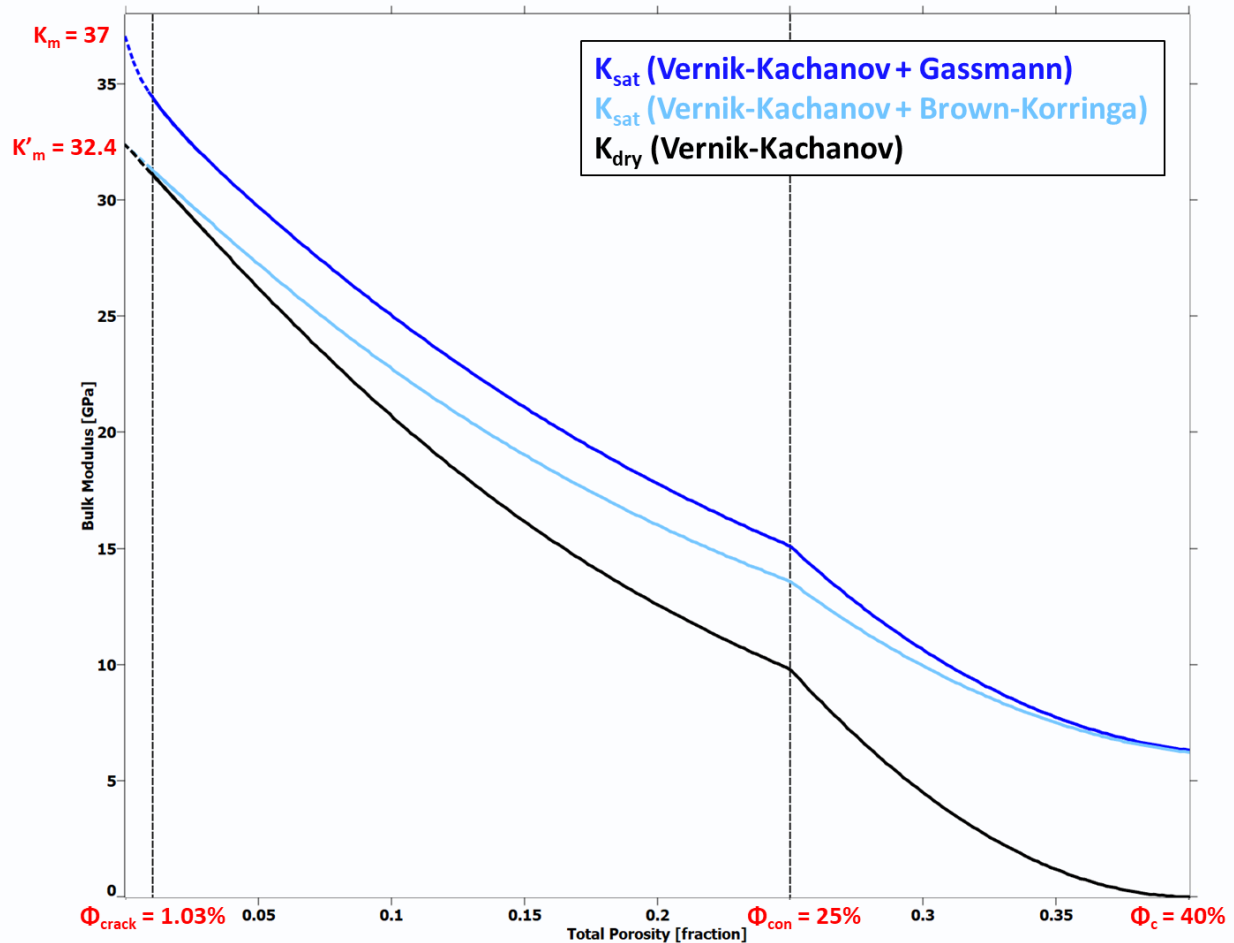


Figure 1: V-K model-based dry bulk modulus (black line) as function of porosity for a sandstone characterized by a relatively low effective stress of 15 MPa and a relatively high crack density, compared to Gassmann (dark blue line) and B-K (light blue line) model-based predictions for a fully brine saturated rock. Predictions below crack porosity (dashed lines) are shown to illustrate the impact of cracks on the zero-porosity end point of the model but cannot happen in reality as cracks can't be closed any further at this effective stress.

Quantification of compliance to Gassmann's assumptions

Although the applicability of Gassmann's theory to a particular rock is a recurrent topic of discussion, few authors have attempted to quantify the deviation of rock behavior to the requirements of Gassmann's model. Amongst these authors, Sahay (2013) defines a micro-inhomogeneity parameter n (referred to simply as a homogeneity parameter hereafter) with a value of 1 for Gassmann-compliant rocks and values that diverge away from 1 for rocks that violate Gassmann's assumptions. According to Müller and Sahay (2014), the potential deformational energy due to a stress applied to a rock "can become partially localized in the interfacial region due to surface roughness or within the bulk part of the solid due to a multiminerall

frame". Both features constitute violations of Gassmann's assumptions. We further suggest that cracks present in a rock also act as focal points for partial localization of deformational energy and therefore contribute to the softening effect as compared to the behavior postulated in Gassmann's theory. Some of this softening may be explained in part by fluid flowing out of the compliant cracks into stiffer pores, a phenomenon often referred to as local or squirt flow effect. By combining equations 3 and 4 from this paper and the generalized poroelasticity framework for micro-inhomogeneous rocks of Müller and Sahay (2016), the homogeneity parameter, that governs the effective pressure dependence of porosity changes, can be conveniently reformulated as a function of measurable effective stress and quantifiable crack density and volumetric pore-shape factor:

$$n \equiv \frac{\psi - \phi}{\beta' - \phi} = \left[1 + \frac{A(v_m) c_2 \exp(-d\sigma)}{p-1} \right]^{-1} \quad (5)$$

where c_2 is the slope of the linear function of porosity used to model η_0 . By definition, n varies according to the difference between ψ , the bulk volume effective pressure coefficient of a micro-heterogeneous rock and β' , the Biot coefficient of a micro-heterogeneous rock defined as $\beta' = 1 - K_d/K'_m$. In the case of micro-homogeneous rocks with no cracks or micro-heterogeneous rocks with cracks subjected to pressures higher than the closure pressure, both coefficients reduce to the familiar form $1 - K_d/K'_m$ and therefore $n = 1$. In contrast, for micro-heterogeneous rocks with cracks subjected to pressures lower than the closure pressure, $K_M < K'_m$ leading to $n < 1$. This effect is illustrated in Figure 2a that shows how larger zero-stress crack density and lower effective stress reduce n in a 23% porosity sandstone with an average pore-shape factor p of 7.1. Figure 2b highlights how, for the same sandstone with a high zero-stress crack density η_0 of 0.66, an increase in effective stress from 5 to 55 MPa reduces its effective crack density and increases its homogeneity parameter, resulting in a state ever closer to Gassmann compliance.

Both Thomsen (2020) and Müller and Sahay (2014) suggest that the assessment of Gassmann's applicability is primarily dependent on the ability to determine Skempton's coefficient based on laboratory quasi-static deformation experiments, which present many challenges of their own and, therefore, are not common. Based on equation 5, we suggest that more routine and straightforward laboratory measurements of velocities vs. stress obtained on dry reservoir rocks are sufficient to calibrate the crack density parameter, derive (optionally) the homogeneity parameter, and apply the more general Brown-Korrington's equation, instead of Gassmann's equation, to perform accurate fluid substitution for a wide range of reservoir rocks under any stress state.

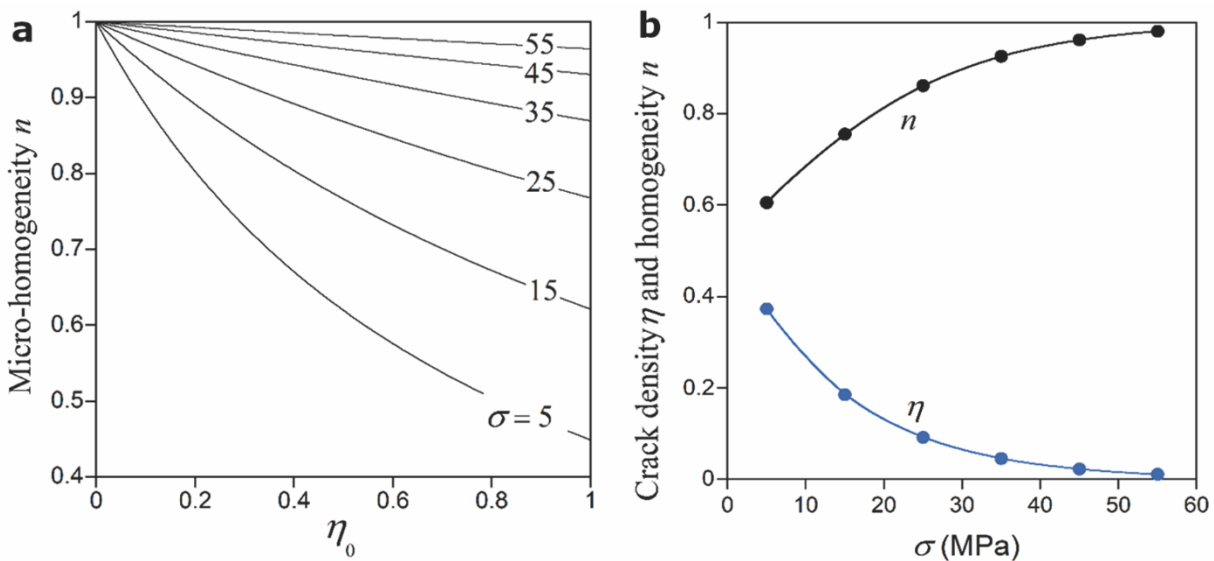


Figure 2: (a) Homogeneity parameter as a function of zero-stress crack density and effective stress (in MPa) in arenite-type 23% porosity sandstone with a pore-shape factor p of 7.1. (b) Evolution of effective crack density and homogeneity parameters as a function of effective stress applied to the same rock as in (a) illustrating how deviation from Gassmann's compliance ($n=1$ or $\eta=0$) decreases with increasing effective stress.

Practical implications in case of a permanent subsea CO₂ storage

Several aspects of CO₂ sequestration in underground reservoirs can potentially result in some of the conditions that lead to significant Gassmann's inaccuracy. First, the injection of CO₂ in the reservoir is accompanied by an increase of pore pressure and therefore a drop of effective stress that will allow existing cracks to open. While this effect will only be transient for sequestration in reservoirs with a pore volume much larger than the projected stored CO₂ volume (saline aquifers for example), the pressure build-up and therefore elastic softening of the reservoir rock could persist in case of reservoirs of smaller size (compartmentalized depleted oil and gas reservoirs for example). In addition, the injection of cold CO₂ in much warmer reservoirs, sometimes resorted to for economic reasons, can lead to a thermal fracturing of the reservoir rock and therefore an increased crack density. However, unlike a pressure increase, this thermal effect is usually limited to the vicinity of injection wells as temperature equilibrium between the host rock and CO₂ is rapidly reached.

For these reasons, it is therefore important to gauge, as part of feasibility studies for CO₂ sequestration projects, the potential evolution of Gassmann's accuracy over time and evaluate whether it would have an impact on the ability to monitor the reservoir with methods sensitive to the elasticity of the rock such as acoustic waves. Such a study was performed based on the Northern Lights dataset from the North Sea where around 1 Mtpa of CO₂ is expected to be pumped into well 31/5-7 situated between the Oseberg and Troll fields. CO₂ will be permanently stored in the Cook and Johansen Jurassic sandstone formations located around 2.6 km below

sea level where CO₂ will be in dense supercritical state. Laboratory tests on core data extracted from the Johansen formation (Griffiths et al., 2012) were used to calibrate the V-K model parameters (Figure 3a). Although difficult to firmly validate in a quantitative manner, the zero-crack density modeled as $\eta_0 = 0.25 + 2\phi$ yields an estimated crack density of 0.11 under in-situ effective stress that seems plausible based on photomicrographs of thin sections of sandstones from the same formation at a nearby well that show evidence of numerous extensively cracked quartz grains (Sundal et al., 2016). Modeling of brine-saturated rock velocities using B-K's equation gives results in accordance with wireline P- and S-wave sonic velocities (Figure 3b) assuming a critical porosity of 40% and a consolidation porosity of 30% which are reasonable values for the Johansen formation.

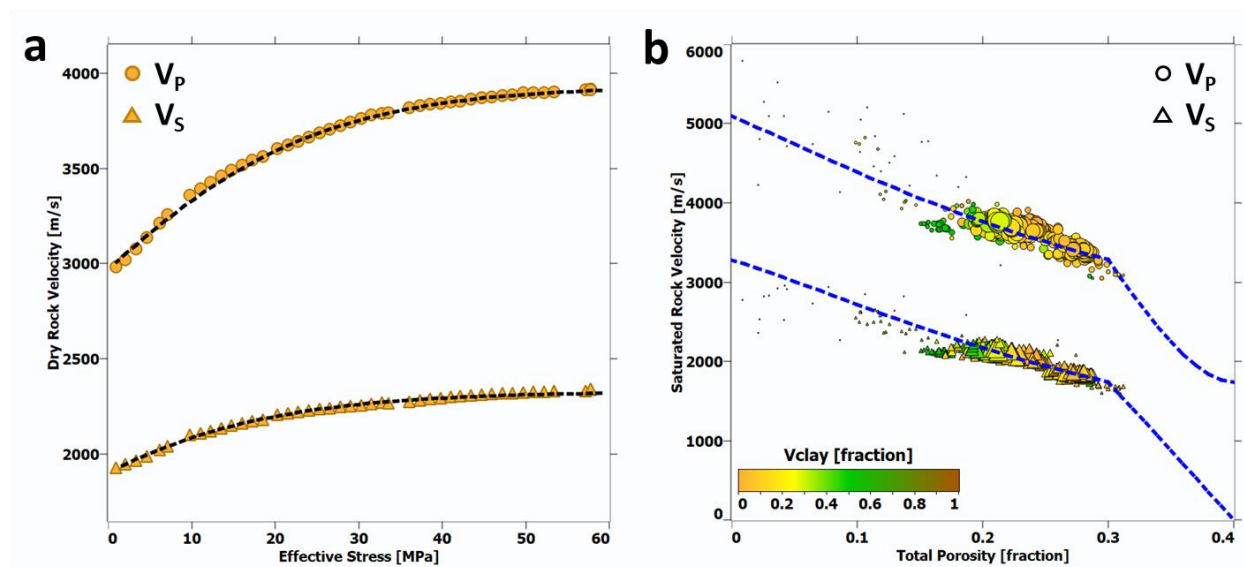


Figure 3: (a) Calibrated V-K model superimposed on dry rock velocities measured in laboratory experiments on core data from the Johansen formation. (b) Same model combined to B-K's equation superimposed on saturated rock velocities from wireline logging of the same brine-filled formation encountered at well 31/5-7.

Application of equation 5 gives micro-homogeneity parameters value of 0.85 (Figure 4). While no significant pressure increase is expected at the site due to the extensive size of the reservoir, we can model the impact a pore pressure build-up of 10 MPa would have on a hypothetical reservoir made of the same rock but with limited size. In this speculative scenario, the effective crack density would increase to 0.23 which would translate into micro-homogeneity parameter value of 0.75 indicating a significant drop in Gassmann's modeling accuracy.

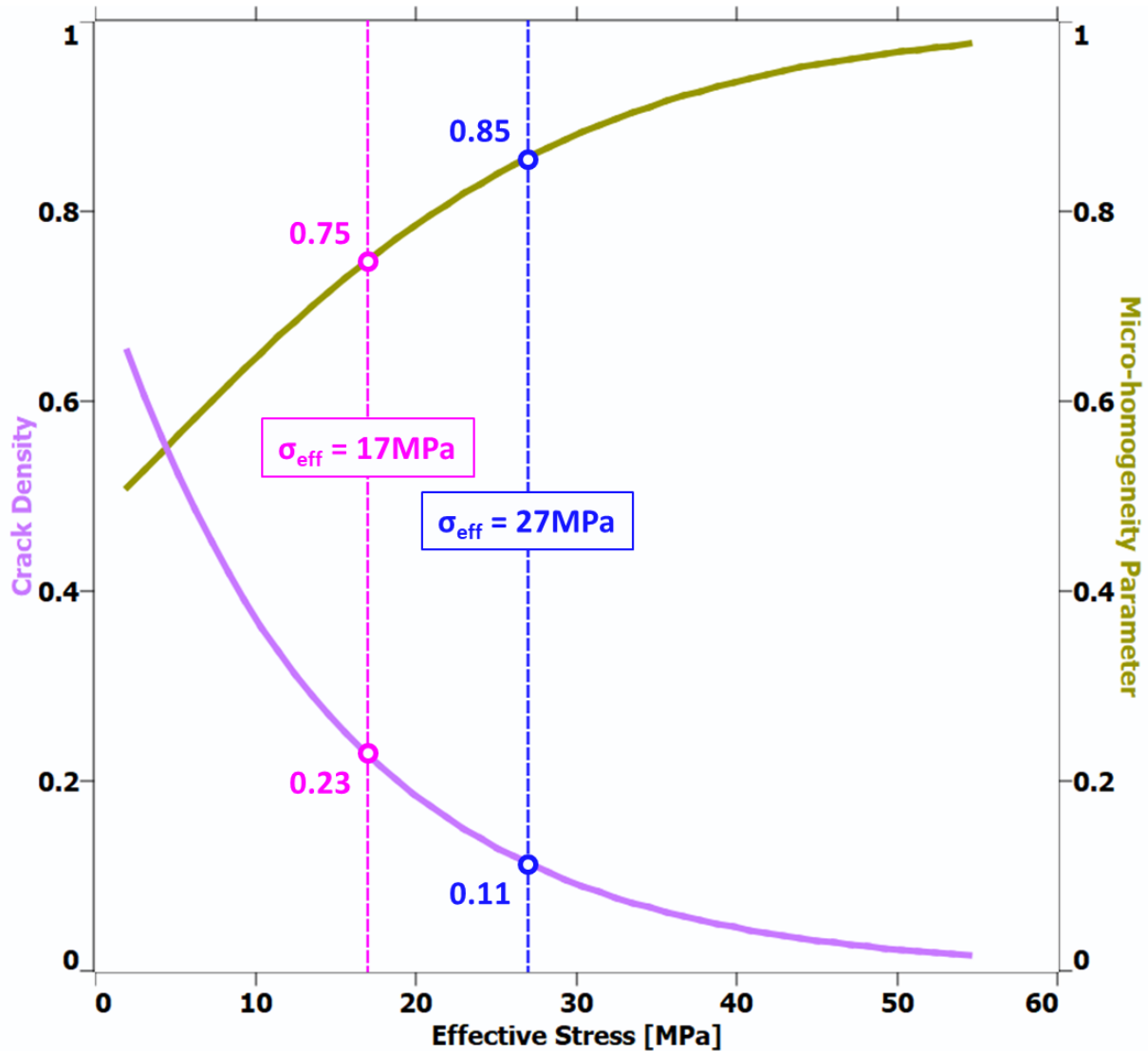


Figure 4: Crack density and micro-homogeneity parameters for a 25% porosity sandstone from the Johansen formation in case of in-situ effective stress (blue) and after a hypothetical pore pressure build-up of 10 MPa due to CO₂ injection (pink).

Figure 5 quantitatively illustrates how this drop of accuracy would translate into larger uncertainties in the context of time-lapse data analysis. It shows that, for a 25% porosity sandstone from the Johansen formation subjected to an in-situ effective stress of 27 MPa, Gassmann's equation overestimates the P-wave impedance of the saturated rock by 1.9% before CO₂ injection and by 1.2% after injection. Should the effective stress drop by 10 MPa, Gassmann's overestimation would roughly double with 4.9% before injection and 2.1% after injection. More importantly, the impedance of the CO₂-saturated rock predicted by Gassmann almost coincides with the impedance of the brine-saturated rock according to B&K indicating a

potential for erroneous interpretation of inverted seismic data. In terms of time-lapse change due to CO₂ injection, the expected impedance drop of 4.2% predicted by Gassmann is only slightly overestimated compared to the drop of 3.5% predicted by B-K. This small inaccuracy appears insignificant when compared to uncertainties associated to other parameters in the forward modeling or various noises that typically pollutes recorded seismic data. But in the hypothetical scenario of a 10 MPa pore pressure increase, the time-lapse impedance drops predicted by Gassmann and B&K would be 5.7% and 3.1% respectively. This overestimation of more than 50% emphasizes that Gassmann's predictions might not be accurate enough in the case of a limited-size reservoir made of a relatively stress-sensitive rock. Depending on the repeatability of the monitoring system in place, the detection threshold could realistically fall in the 4 to 5% of P-wave impedance change in which case one would expect to detect a change based on Gassmann's predictions whereas, in practice, and according to the more accurate B&K equation, no change might be detectable. This larger error in a limited-size depleted field is compounded by the fact that, compared to a storage in saline aquifer, a smaller change of P-wave impedance is expected due to the presence of residual natural gas in the pore space. Although based on a hypothetical scenario in this example, this kind of considerations are highly relevant for CO₂ containment monitoring where tracking of plume conformance and timing of leak detection are of utmost importance.

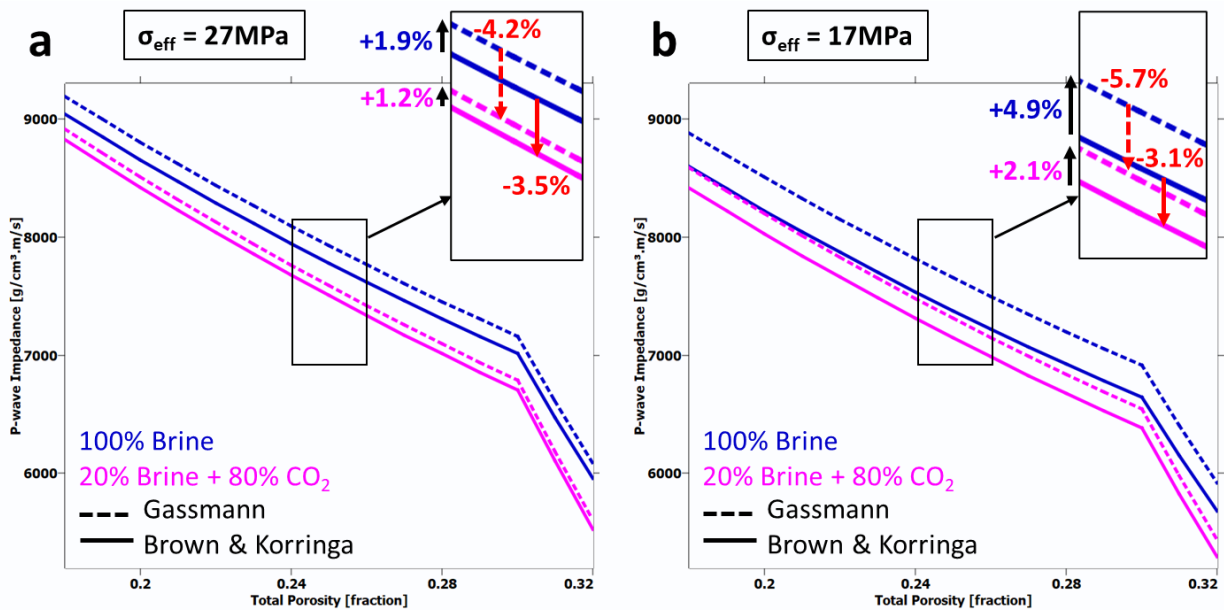


Figure 5: Difference in saturated rock P-wave impedance predicted by Gassmann (dashed lines) and B-K (solid lines) based models for brine (blue) and 80% CO₂ + 20% brine (pink) scenarios for a 25% porosity sandstone from the Johansen formation subjected to (a) in-situ effective stress or (b) a hypothetical reduced effective stress caused by a pore pressure build-up of 10 MPa due to CO₂ injection. Time-lapse changes predicted by both models are indicated in red in the zoomed insets.

Conclusions

The application of Gassmann's equation to estimate fluid effects on P-wave velocity in reservoir rocks can be substantially inaccurate for porous rocks with moderate to high crack density. We also show that, as a consequence, Gassmann's prediction error is directly related to the stress sensitivity of the reservoir rock. As practical operations in CO₂ sequestration project can lead to low effective stress and high crack density, we therefore highly recommend checking that the reservoir rock comply to Gassmann's assumptions as part of any feasibility study. A simple metric based on laboratory-measured stress-dependent dry rock velocities is suggested to rapidly assess Gassmann's applicability. Extrapolating from the results of this study, Gassmann's predictions are expected to be accurate enough for most CO₂ sequestration modeling case studies especially when CO₂ is injected in large saline aquifer reservoirs. In case of storage in a compartmentalized depleted field, where a smaller time-lapse impedance change and a larger increase of pore pressure can be expected, the Vernik-Kachanov model and the more general Brown-Korrington fluid substitution equation should be contemplated as a more accurate alternative.

Acknowledgements

We thank Viridien for granting permission to publish this work. We are also extremely grateful to the Northern Lights project partners for making the Eos dataset publicly available and in so allowing the advance of scientific research on critical topics such as CO₂ capture and storage.

References

- Benveniste, Y., 1987, A new approach to the application of Mori-Tanaka's theory in composite materials: *Mechanics of Materials*, **6**, no. 2, 147-157, [https://doi.org/10.1016/0167-6636\(87\)90005-6](https://doi.org/10.1016/0167-6636(87)90005-6).
- Biot, M.A., 1941, General theory of three-dimensional consolidation: *Journal of Applied Physics*, **12**, no. 2, 155-164, <https://doi.org/10.1063/1.1712886>.
- Brown, R. J. S., and J. Korrington, 1975, On the dependence of the elastic properties of a porous rock on the compressibility of the pore fluid: *Geophysics*, **40**, 608-616, <https://doi.org/10.1190/1.1440551>.
- Duranti, L., 2018, On the homogeneity of poroelastic media: Experimental measurements: Expanded Abstracts, 88th Annual International Meeting, SEG, <https://doi.org/10.1190/segam2018-2998972.1>.
- Griffiths, L., N. Thompson, H. Smith, L. Grande and E. Skurtveit, 2012, Rock mechanical testing of core from Eos CCS validation well, Trondheim Carbon Capture and Storage Conference.
- Kachanov, M., I. Tsukrov and B. Shafiro, 1994, Effective moduli of solids with cavities of various shapes: *Applied Mechanics Reviews*, **47**, no. 1S, S151-S174, <https://doi.org/10.1115/1.3122810>.
- Mavko, G., T. Mukerji, and J. Dvorkin, 2009, *The rock physics handbook: Tools for seismic analysis of porous media*, 2nd ed: Cambridge University Press, <https://doi.org/10.1017/CBO9780511626753>.
- Müller, T. M., and P. N. Sahay, 2014, Skempton's coefficient and its relation to the Biot bulk coefficient and micro-inhomogeneity parameter: Expanded Abstracts, 84th Annual International Meeting, SEG, <https://doi.org/10.1190/segam2014-0446.1>.
- Müller, T. M., and P. N. Sahay, 2016, Generalized poroelasticity framework for micro-inhomogeneous rocks: *Geophysical Prospecting*, **64**, no. 4, 1122-1134, <https://doi.org/10.1111/1365-2478.12392>.
- Sahay, P. N., 2013, Biot constitutive relation and porosity perturbation equation: *Geophysics*, **78**, no. 5, L57-L67, <https://doi.org/10.1190/geo2012-0239.1>.

- Sundal, A., J.P. Nystuen, K-L. Rørvik, H. Dypvik and P. Aagard, 2016, The Lower Jurassic Johansen Formation, northern North Sea – Depositional model and reservoir characterization for CO₂ storage, *Marine and Petroleum Geology*, **77**, 1376-1401, <https://doi.org/10.1016/j.marpetgeo.2016.01.021>.
- Thomsen, L., 2020, A logical error in Gassmann poroelasticity: 90th Annual International Meeting, SEG, 2429–2933, <https://doi.org/10.1190/segam2020-3424536.1>.
- Thomsen, L., 2021, The logical error in Gassmann poroelasticity: Consistency with effective medium theory: 1st International Meeting for Applied Geoscience & Energy, SEG, <https://doi.org/10.1190/segam2021-3580471.1>.
- Vernik, L., and M. Kachanov, 2010, Modeling elastic properties of siliciclastic rocks: *Geophysics*, **75**, no. 6, E171–E182, <https://doi.org/10.1190/1.3494031>.
- Vernik, L., 2016, Seismic petrophysics in quantitative interpretation, SEG, <https://doi.org/10.1190/1.9781560803256>.